ChemistryOpen

Communications
doi.org/10.1002/open.202000106

Chemistry Europe
European Chemical
Societies Publishing

Self-Assembly Anisotropic Magnetic Nanowire Films Induced by External Magnetic Field

Muhammad Hassan[+], Hui-Juan Zhan[+], Jin-Long Wang, Jian-Wei Liu,* and Jia-Fu Chen*[a]

Self-assembly generated materials induced by an external magnetic field have attracted considerable interest following the development of nanodevices. However, the fabrication of macroscopic and anisotropic magnetic films at the nanoscale remains a challenge. Here, anisotropic magnetic films are successfully prepared using a solution-based nanowire assembly strategy under a magnetic field. The assembly process is manipulated by changing the thickness of silica shell coated on the surface of magnetic nanowires. The anisotropic magnetic films show highly anisotropic magnetization under different angles of magnetic field and better magnetization properties than that of disordered magnetic films. The well-defined nanowire arrays enable magnetization anisotropic property which may be useful in the magnetic energy conversion technologies and biomedical sciences which lie far beyond those achievable with traditional magnetic materials.

Nanowire (NW) hierarchical structures generated upon self-assembly have endowed the programmable availability of suitable one-dimensional (1D) nano-building blocks and play a vital role in not only understanding of many natural structures at all scales but also offering an effective elucidation for the problem of fabricating structures beyond molecular levels.[1] In comparison to NW with a disordered statement, well-designed NW assemblies have the advantage of possessing collective properties due to interactions and synergy effect between the NWs beyond the individual 1D building blocks.[2] A magnetic field provides a vector field that describes the magnetic influence on electrical currents and magnetized materials, which is used by many animals for orientation and navigation including homing and long-distance migration. Inspired by these magnetosensing behaviors in nature, self-assembly

induced by an external magnetic field has attracted explosive attention owing to their unique structures, interesting properties and potential for novel applications.[3] Due to the low aspect ratio of the nanoparticle building blocks, these assembled structures show a limited magnetization anisotropy.

Some homing animals can return to their loft after long-distance displacement to unfamiliar release sites. Anisotropic magnetic field in the brain is thought to be one of the most common abilities of these animals for orientation and navigation by perceiving Earth's magnetic field.[4] Although the research field of anisotropic magnetic field has attracted plenty of attention, macroscopic fabrication of anisotropic magnetic films at nanoscales still remains a big challenge.

Herein, we report a simple solution-based bottom-up self-assembly process induced by external magnetic field to fabricate well-defined magnetic NW films. Rational thickness of SiO_2 was coated on the surface of the magnetic NWs to balance the magneto-sensitivity between the internal adjacent magnetic NWs and the interaction between NWs and the external magnetic field. After placing the NW solution in an external magnetic field, each part of the NW gets a force parallel to the field direction, resulting in an ordered NW film. The obtained ordered SiO_2-coated Fe_3O_4—AgNWs films exhibit a better magnetization property as compared to the disordered NWs films and more interestingly, the NW films show highly anisotropic magnetization.

In Figure 1a, the procedure for the NW assembly process in a magnetic field is shown. To regulate the self-assembly of magnetic nanomaterials, a reasonable composition design was

[a] *Dr. M. Hassan,[+] H.-J. Zhan,[+] Dr. J.-L. Wang, Prof. J.-W. Liu, Prof. J.-F. Chen*
    Division of Nanomaterials & Chemistry
    Hefei National Laboratory for Physical Sciences at the Microscale
    Department of Chemistry
    University of Science and Technology of China
    Hefei 230026 (China)
    E-mail: jwliu13@ustc.edu.cn
    *   jfchen@ustc.edu.cn*
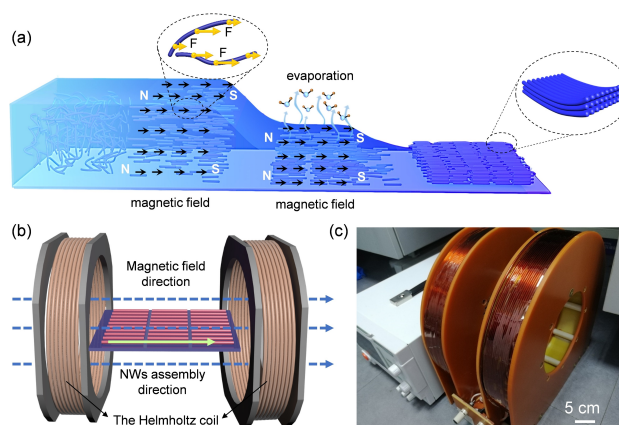[+] *These authors contributed equally to this work.*

Figure 1. a) Schematic illustration of the proposed assembly procedure. b) The diagram of the magnetic assembly of NWs assisted by the Helmholtz coil. c) The photos of the direct-current power system (left) and the Helmholtz coil (right).

ChemistryOpen

Communications
doi.org/10.1002/open.202000106

Chemistry Europe
European Chemical
Societies Publishing

carried out to improve the assembly process. Figure S1 in the Supporting information presents the typical transmission electron microscopy (TEM) image of Fe_3O_4–AgNWs that was synthesized by the modified solvothermal process,[5] showing the homogenous distribution of Fe_3O_4 nanoparticles around AgNWs (inset of Figure S1). The core-shell NW architecture endows their response under the external magnetic field stimulation. In the absence of the silica shell, strong dipolar interaction is dominant, and it will affect the assembly process and hinder the formation of a uniform NW film.[6] Whereas, too much SiO_2 coating (the thickness) will result in an insensitive response to the external field. In details, the thickness of the SiO_2 shell was easily controlled by changing mainly two parameters, including reaction time and concentration of Tetraethyl orthosilicate (TEOS) with optimal SiO_2 shell thickness, well-defined structures can be easily obtained in the assembly process (Figure S2 and Figure S3, Supporting information). Figure S4 in the Supporting information gives the relationship between the SiO_2 thickness with reaction time and concentration of TEOS, showing the deposition of SiO_2 increased linearly with both reaction time and concentration of TEOS, similar to the previous work.[7] The HRTEM image of SiO_2-coated Fe_3O_4–AgNWs revealed the crystalline nature of AgNW and Fe_3O_4 nanoparticles (Figure S5a, Supporting information). The elemental composition confirmed by energy-dispersive spectroscopy (EDS) is presented in figure S5b in the Supporting information, indicating the relative peaks of Ag, Fe and Si. An additional piece of evidence was confirmed by EDS mapping of Ag (magenta), Fe (green) and Si (yellow) (Figure S6, Supporting information). These results revealed the homogenous distribution of involved elements around AgNW. The magnetic properties of the SiO_2-coated Fe_3O_4–AgNWs were explored by a superconducting quantum interference device (SQUID) at 300 K (Figure S7, Supporting information). The saturation magnetization of Fe_3O_4–AgNWs and SiO_2-coated Fe_3O_4–AgNWs were approximately 36, and 23 emu/g, respectively, showing superparamagnetic behavior at room temperature. Moreover, in case of SiO_2-coated Fe_3O_4–AgNWs lower values of magnetization was obtained, showing that the magnetic properties can be tuned easily by altering thickness of SiO_2 layer around Fe_3O_4–AgNWs.

The field-induced alignment and the self-assembly study of the SiO_2-coated Fe_3O_4–AgNWs were investigated by establishing an experimental setup in which a transparent polycarbonate (PC) film is placed in a container and the uniform magnetic field is offered by the central zone of a Helmholtz coil (Figure 1b, c). Droplets of the SiO_2-coated Fe_3O_4–AgNWs suspended in deionized water were released onto a PC substrate under the magnetic field. The magnetic force generated in the direction of magnetic field lines translocated the SiO_2-coated Fe_3O_4–AgNWs and upon drying the NWs were aligned with the field direction between the Helmholtz coils. The magnetic field strong components generated forces in X-direction that produce a torque in the plane parallel to the aligned NWs.[8] The position of the sample was arranged to achieve the appropriate combination of the components of the magnetic field vector.

Moreover, the capillary forces between SiO_2-coated Fe_3O_4–AgNWs resulted in the closed packing of NWs.[9]

According to the Biot-Savart law, the magnetic field ($\vec{B}$) generated by the current carrying wires in the Helmholtz coil can be described as:[10]

$$\vec{B}(\vec{r}) = \frac{\mu_0}{4\pi} \int_C \frac{Id\vec{l} \times \vec{r}}{\|\vec{r}\|3} \tag{1}$$

Where μ_o is the permeability of free space $= 4\pi \times 10^{-7}$ H/m, C is the path of the current carrying wire, I is the current intensity, $d\vec{l}$ is the vector along the wire path and $\vec{r}$ is the vector from the wire element to the point. From the formula (1), the theoretical modeling has predicted that the Helmholtz coil has a drastically lower magnetic field gradient error ($< 1\%$) when compared to permanent magnet, and we can easily change the magnetic field intensity by only changing the current intensity of the carrying wires. Figure 2a shows the optical image of magnetic assembly of SiO_2-coated Fe_3O_4–AgNWs films which is very uniform. Nearly all the NWs aligned along the direction of the external field. Besides of the ordered NW arrays, we can fabricate more complicated NW structures. As we knew, the formation of regular mesh-like mesostructures of the order of several nanometers is difficult which needs high temperature and a special substrate.[11] Here, we introduce our method to fabricate two layers of periodic NW films with designable nanomesh. Figure 2b,c shows the mesh structure of SiO_2-coated Fe_3O_4–AgNWs, fabricated in two consecutive steps. After deposition of the first layer of aligned NWs on the PC substrate, the same step was repeated by rotating the magnetic field at 90° that created the second layer of aligned NWs on the surface, resulting in a mesh structure.

The ordered NW structures can be quantitatively estimated by statistical analysis with Image-J software using the orienta-
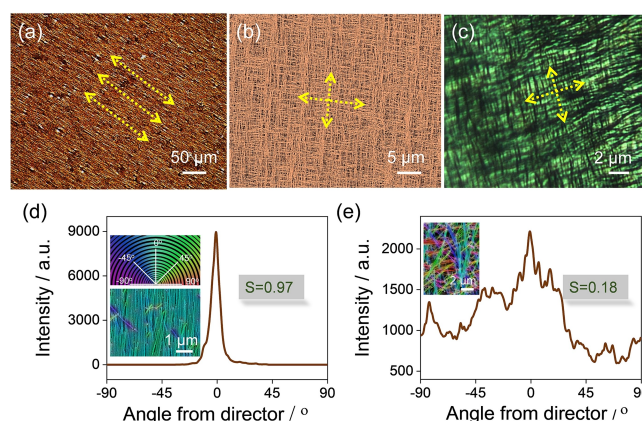

Figure 2. a) Optical image of magnetic assembly of SiO_2-coated Fe_3O_4–AgNWs film. b) SEM image of aligned SiO_2-coated Fe_3O_4–AgNWs film mesh-type structure. c) Optical image of aligned SiO_2-coated Fe_3O_4–AgNWs film mesh-type structure. d) Distribution of the ordered SiO_2-coated Fe_3O_4–AgNWs at angle θ, inset: orientation analysis of the aligned SiO_2-coated Fe_3O_4–AgNWs film with the color-coding. e) Orientation analysis of the disordered SiO_2-coated Fe_3O_4–AgNWs film with the plot of alignment intensity distributions. inset: the color-coding of disordered SiO_2-coated Fe_3O_4–AgNWs film naturally evaporated without the external magnetic field.

ChemistryOpen

Communications
doi.org/10.1002/open.202000106

Chemistry Europe
European Chemical
Societies Publishing

tion parameter S ($0 \leq S \leq 1$).[12] The output of this analysis was measured in terms of the distribution of space-correlation alignment intensity as a function of angle and this local orientation is color-coded (different colors denote different alignment directions). The S value was determined by averaging over the angle as

$$S = 2 < \cos^2\theta > -1 \qquad (2)$$

Where θ is the angle with the main director. The resultant orientational parameter S can change from 0 (low orientation) to 1 (high orientation). Figure 2d shows the histogram of orientations and the orientation parameter (S) was computed according to the equations (2) that correspond to 0.97, exhibiting an excellent degree of alignment in NWs. The inset of Figure 2d shows the color image with the orientation being encoded in the color description, revealing that most NWs were aligned in one direction with the color appearing near to 0°. In the case of disorder NWs film, multi colors image was obtained with a decrease in S value from 0.97 to 0.18 (Figure 2e).

The choice of solvent for field-induced self-assembly is quite important as the magnetic assembly is strongly influenced by the effect of capillary forces that occur in samples during drying. Three kinds of solvents (water, isopropanol and butanol) were selected to disperse the SiO_2-coated Fe_3O_4–AgNWs and carry out the experiment. Figure S8 in the Supporting information shows that in case of water as the solvent, a potential ordering was observed (S = 0.97), whereas by changing solvents to IPA and butanol NWs agglomeration occurred during the assembly process (Figure S9, Supporting information), resulting in a decrease in ordering value from 0.97 to 0.92 respectively. Solvents may affect the assembly process in the following ways. Firstly, the electrostatic interaction between solvent and magnetic NWs that arose from the hydroxyl groups of solvent and SiO_2 shell makes the good dispersion of NWs in the solvent. And water has more hydroxyl groups and better affinity than isopropanol and butanol. Besides, water evaporates more slowly, which decreases adverse influence on the assembly process because of the disturbance caused by the quick solvent evaporation. Moreover, the density of water is larger than that of isopropanol and butanol, NWs experience more buoyancy and are less likely to sink to the bottom, which is beneficial for the assembly process.

Furthermore, we explored the use of an additional SiO_2 layer to tune magnetic interactions and magnetic field-driven self-assembly process. Figure S10 in the Supporting information shows the effect of SiO_2 coating on NWs magnetic assembly. In case of without SiO_2 coating, the dipolar interaction is very strong that binds the system in a kinetically arrested state and hampers the formation of an equilibrium structure. Hence in the absence of SiO_2 shell, a film with a relative lower S value (0.91) was obtained (Figure S11a, Supporting information). However, with 13 nm SiO_2 coating of Fe_3O_4–AgNWs (Figure S11b, Supporting Information), well-defined structures are prominent with the S value increasing to 0.97, showing the projection of optimal shell thickness to well-defined structure. Additionally, the further increase in SiO_2 coating from 13 nm to

38 nm leads to the weakening of dipolar interaction and the influence of applied magnetic field was not strong enough to tune the NWs in preferred direction,[6] resulting decrease in S value from 0.97 to 0.71 and disordered NWs film was obtained as shown in Figure S11c–e in the Supporting information.

The dipolar coupling between magnetic SiO_2-coated Fe_3O_4–AgNWs in ordered film induces magnetic shape anisotropy, and therefore subjected to the artificial magnetic field perception, inspired by bioinspired magnetic field perception system.[3d] As shown in Figure 3a, it describes the preparation procedure for ordered and disordered NW films for the magnetic measurement. The field dependence of magnetization measured at 300 K for both aligned and random NWs film samples is presented in Figure 3b, showing an increase in magnetization for the aligned NWs film (red loop) with increasing applied magnetic field as compared to random one (blue loop). These results suggested that the cooperative response of SiO_2-coated Fe_3O_4–AgNWs is more sensitive to magnetic field due to anisotropic alignment of NWs in ordered film.[13] The SiO_2-coated Fe_3O_4–AgNWs exhibit no magnetization under zero applied magnetic field, however, on applying the magnetic field, the magnetic moments can be aligned and the magnetization intensity is calculated by the integrating magnetic moments along the magnetic field direction (B). Figure 3c shows the maximum value of magnetization intensity in the case of the parallel direction of the applied magnetic field (B) to the axis of the aligned NWs film. While, the magnetization intensity decreases by changing the direction of applied
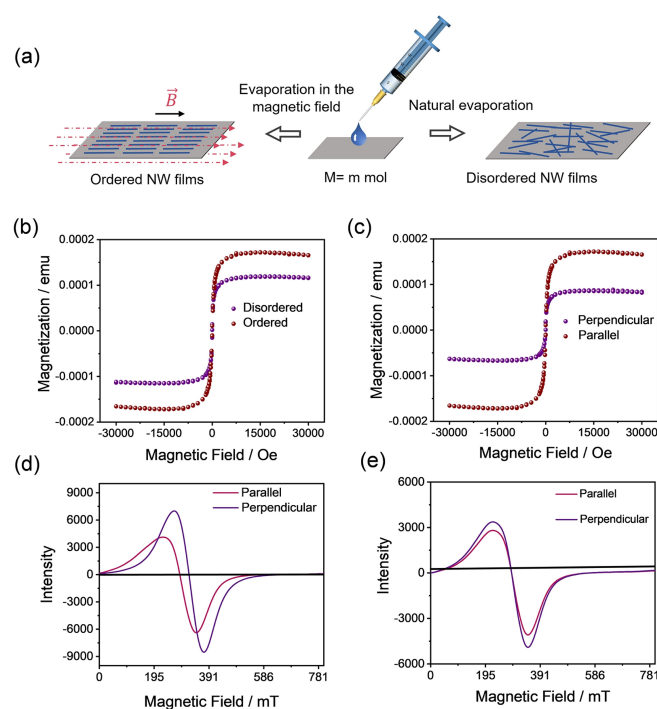
Figure 3. a) Schematic representation of the preparation and quantification procedures of ordered and disordered NW films. b) Magnetic properties of ordered and disordered SiO_2-coated Fe_3O_4–AgNWs film. c) Magnetic properties of aligned SiO_2-coated Fe_3O_4–AgNWs film at parallel and perpendicular direction of the applied magnetic field. EPR spectra of d) ordered NWs film and e) disordered NWs film.

ChemistryOpen

Communications
doi.org/10.1002/open.202000106

Chemistry Europe
European Chemical
Societies Publishing

magnetic field to orthogonal direction with the axis of aligned NWs film. The ratio of maximum and minimum value of magnetization M_{max}/M_{min} under deferent directions of the applied magnetic field gives the idea to evaluate the magnetic anisotropy of aligned NWs and measured as 2.01 in our system. Hence, for magnetic perception applications, this anisotropic magnetization property benefits an effective rout to measure the magnetization dependence of aligned NWs at different angle θ. To further demonstrate the magnetic anisotropy as a result of NWs alignment, electron paramagnetic resonance (EPR) was performed with the condition of the parallel and perpendicular magnetic field. Figure 3d, e shows the EPR spectra for disordered and ordered NWs films by applying the magnetic field parallel and perpendicular to the samples. For randomly distributed NWs no resonance shift in EPR spectrum was observed, indicating no angular dependence in case of disordered NWs film. However, the ordered NWs film presented a shift of the EPR spectrum that is comparatively a larger resonance field when the magnetic field is applied perpendicular to the chain axis and smaller resonance field in case of parallel axis, revealing the angular dependence for the ordered NWs film that points towards the existence of uniaxial magnetic anisotropy with its axis parallel to the aligned NWs axis.[14]

In summary, we demonstrated the magnetic assembly SiO_2-coated Fe_3O_4—AgNWs having tunable magnetic properties with good orientational ordering. The NWs were synthesized by the heteroaggregation of SiO_2 and Fe_3O_4—AgNWs. The magnetic field aligned the SiO_2-coated Fe_3O_4—AgNWs with their major axes parallel to the field direction. The optimized parametric study allowed us to achieve the magnetic assembly of SiO_2-coated Fe_3O_4—AgNWs with good ordering. The superparamagnetic nature and high-aspect-ratio characteristic of assembled SiO_2-coated Fe_3O_4—AgNWs film possessed the superior magnetization properties and highly anisotropic magnetization under different angle magnetic field as compared to disordered NWs film. These properties facilitate the successful implication of our assembled films to study the enhancement in properties in the application of magnetocaloric effect and magnetic-field-perception system.

Experimental Section

Synthesis of Fe₃O₄—AgNWs

Fe_3O_4—AgNWs were prepared by a modified polyol process.[5] Briefly, AgNWs (0.5 g) was added into of PVP (8%) ethylene glycol solution (18 mL) and kept on stirring for 45 min at 50°C. Then ferric nitrate (0.45 g) and sodium acetate anhydrous (3 g) were added in diethylene glycol (66 mL) and stirred for a homogenous mixture. Afterward, the two solutions were mixed in a three-neck round bottom flask and held on vigorous stirring at 60°C under N₂ flow for 1 h to make a homogenous distribution. The mixture was closed in a 100 mL Teflon-lined stainless-steel autoclave and maintained at 200°C for 10 h. After the reaction is over, the products were washed several times with acetone and centrifuged in ethanol and water at 4000 rpm to get the final product.

Synthesis of SiO₂-coated Fe₃O₄—AgNWs

The SiO_2-coated Fe_3O_4—AgNWs were prepared by a modified Stöber method.[15] In a typical process, Fe_3O_4—AgNWs (25 mg) were dispersed in a mixture of 2-propanol (30 mL) and water (3 mL) in a round-bottomed flask (50 mL) immersed in a constant temperature bath of 35°C. Under continuous magnetic stirring, ammonia solution (400 μL, 30%) and of TEOS (120 μL, Aldrich) were sequentially added to this system and kept for stirring at different time intervals to obtain SiO_2 coating of different thickness. After washing and centrifuge at 4000 rpm with ethanol and water, the final product was redispersed in water.

Characterization Methods

Morphology was determined by SEM images taken on a Zeiss Supra 40 SEM at an acceleration voltage of 5 kV and TEM images collected on a Hitachi H7650 transmission electron microscope operated at an acceleration voltage of 120 kV with Change Coupled Device (CCD) imaging system. High-resolution transmission electron microscope (HRTEM) observations were conducted on JEOL-2010F with an acceleration voltage of 200 kV. The optical images were taken by an optical microscope (VHM2000, Shanghai Weihan Optoelectronic technology co., LTD). Thermal images were recorded by a thermal imager VarioCAM hr head 680 (InfraTec GmbH). Magnetization curves were recorded at 300 K by applying field parralel and perpendicular to plane of the substrate along a specific direction by using a SQUID, a quantum design MPMS XL-7 magnetometer. Electron paramagnetic resonance (EPR) experiments were performed in an Electron Paramagnetic Resonance spectrometer (JES-FA200). The magnetocaloric effect was measured by inserting NWs containing PC substrate under an alternating current (AC) magnetic field that was generated by 4.5 cm coil appartus (Shenzhen Shuangping power supply technology Co., Ltd., China) at a medium frequency of (375 KHz) for 10 min.

The assembly of Magnetic NWs

The uniform magnetic field was offered by a Helmholtz coil (Hangzhou pafei technology co., LTD) with a direct-current power system (eTM-6015C, MRS Sci&Tech). When the current was 10 A, the magnetic field intensity of the central zone (60×60×60 mm) of the Helmholtz coil was about 40 mT which was measured by a Teslameter (changsha Tunkia co., LTD). The substrate was placed on the central zone of the Helmholtz coil, and the magnetic NWs solution dropped on the substrate. After the solvent evaporates, the assembled magnetic NWs film was obtained.

Conflict of Interest

The authors declare no conflict of interest.

ChemistryOpen

Communications
doi.org/10.1002/open.202000106

Chemistry Europe
European Chemical
Societies Publishing

[1] a) J.-W. Liu, H.-W. Liang, S.-H. Yu, *Chem. Rev.* **2012**, *112*, 4770; b) U. G. Wegst, H. Bai, E. Saiz, A. P. Tomsia, R. O. Ritchie, *Nat. Mater.* **2015**, *14*, 23; c) G. M. Whitesides, B. Grzybowski, *Science* **2002**, *295*, 2418; d) J.-W. Liu, S.-H. Yu, *Natl. Sci. Rev.* **2015**, *2*, 392.

[2] a) J. L. Wang, M. Hassan, J. W. Liu, S. H. Yu, *Adv. Mater.* **2018**, *30*, 1803430; b) C. Yan, T. Wang, *Chem. Soc. Rev.* **2017**, *46*, 1483–1509; c) W. Liu, S. W. Lee, D. Lin, F. Shi, S. Wang, A. D. Sendek, Y. Cui, *Nat. Energy* **2017**, *2*, 17035; d) J.-W. Liu, J. Xu, Y. Ni, F.-J. Fan, C.-L. Zhang, S.-H. Yu, *ACS Nano* **2012**, *6*, 4500.

[3] a) B. Bharti, A.-L. Fameau, M. Rubinstein, O. D. Velev, *Nat. Mater.* **2015**, *14*, 1104; b) A. F. Demirörs, P. P. Pillai, B. Kowalczyk, B. A. Grzybowski, *Nature* **2013**, *503*, 99; c) T. Udayabhaskararao, T. Altantzis, L. Houben, M. Coronado-Puchau, J. Langer, R. Popovitz-Biro, L. M. Liz-Marzán, L. Vuković, P. Král, S. Bals, *Science* **2017**, *358*, 514–518; d) X. Jiang, J. Feng, L. Huang, Y. Wu, B. Su, W. Yang, L. Mai, L. Jiang, *Adv. Mater.* **2016**, *28*, 6952.

[4] a) X. Y. Jiang, J. G. Feng, L. Huang, Y. C. Wu, B. Su, W. S. Yang, L. Q. Mai, L. Jiang, *Adv. Mater.* **2016**, *28*, 6952; b) H. Mouritsen, *Nature* **2018**, *558*, 50.

[5] A. R. Rathmell, M. Nguyen, M. Chi, B. J. Wiley, *Nano Lett.* **2012**, *12*, 3193.

[6] V. Malik, A. Pal, O. Pravaz, J. J. Crassous, S. Granville, B. Grobety, A. M. Hirt, H. Dietsch, P. Schurtenberger, *Nanoscale* **2017**, *9*, 14405.

[7] Y. Yin, Y. Lu, Y. Sun, Y. Xia, *Nano Lett.* **2002**, *2*, 427.

[8] Z. Nie, A. Petukhova, E. Kumacheva, *Nat. Nanotechnol.* **2010**, *5*, 15.

[9] T. Ding, K. Song, K. Clays, C. H. Tung, *Adv. Mater.* **2009**, *21*, 1936.

[10] I. Nelson, T. A. Ogden, S. Al Khateeb, J. Graser, T. D. Sparks, J. J. Abbott, S. E. Naleway, *Adv. Eng. Mater.* **2019**, *21*, 1801092.

[11] a) M. Corso, W. Auwarter, M. Muntwiler, A. Tamai, T. Greber, J. Osterwalder, *Science* **2004**, *303*, 217; b) J. W. Liu, J. H. Zhu, C. L. Zhang, H. W. Liang, S. H. Yu, *J. Am. Chem. Soc.* **2010**, *132*, 8945.

[12] a) J. J. Armao IV, I. Nyrkova, G. Fuks, A. Osypenko, M. Maaloum, E. Moulin, R. Arenal, O. Gavat, A. Semenov, N. Giuseppone, *J. Am. Chem. Soc.* **2017**, *139*, 2345; b) R. Rezakhaniha, A. Agianniotis, J. T. C. Schrauwen, A. Griffa, D. Sage, C. v. Bouten, F. Van de Vosse, M. Unser, N. Stergiopulos, *Biomech. Model. Mechanobiol.* **2012**, *11*, 461; c) C. A. Schneider, W. S. Rasband, K. W. Eliceiri, *Nat. Methods* **2012**, *9*, 671.

[13] E. Myrovali, N. Maniotis, A. Makridis, A. Terzopoulou, V. Ntomprougkidis, K. Simeonidis, D. Sakellari, O. Kalogirou, T. Samaras, R. Salikhov, *Sci. Rep.* **2016**, *6*, 37934.

[14] D. Toulemon, M. V. Rastei, D. Schmool, J. S. Garitaonandia, L. Lezama, X. Cattoën, S. Bégin-Colin, B. P. Pichon, *Adv. Funct. Mater.* **2016**, *26*, 2454.

[15] J. Ge, Y. Hu, T. Zhang, Y. Yin, *J. Am. Chem. Soc.* **2007**, *129*, 8974.